description, with the implicit admission that diffraction data may well be unable to provide an unambiguous result.*

* Lists of structure factors for all five compounds, U_{ij}'s for compounds (2), (3) and (4) and assumed H-atom coordinates for compound (2) have been deposited with the IUCr (Reference: BU311). Copies may be obtained through The Managing Editor, International Union of Crystallography, 5 Abbey Square, Chester CH1 2HU, England.

References

BARTCZAK, T. J. & YAGBASAN, R. (1991). *Acta Cryst.* C**47**, 1750–1752.

COYER, M., HERBER, R. H. & COHEN, S. (1991). *Acta Cryst.* C**47**, 1376–1378.

DUNITZ, J. D. (1979). *X-ray Analysis and the Structure of Organic Molecules*, pp. 208–209. Ithaca and London: Cornell Univ. Press.

ERMER, O. & DUNITZ, J. D. (1970). *Acta Cryst.* A**26**, 163.

KAMOUN, S., JOUINI, A., DAOUD, A., DURIF, A. & GUITEL, J. C. (1992). *Acta Cryst.* C**48**, 133–135.

MARSH, R. E. (1981). *Acta Cryst.* B**37**, 1985–1988.

MARSH, R. E. (1986). *Acta Cryst.* B**42**, 193–198.

OKADA, A., KOBAYASHI, K., ITO, T. & SAKURAI, T. (1991). *Acta Cryst.* C**47**, 1358–1361.

SCHOMAKER, V. & MARSH, R. E. (1979). *Acta Cryst.* B**35**, 2331–2336.

WOPERSNOW, W. & SCHUBERT, K. (1976). *J. Less-Common Met.* **48**, 79–87.

Acta Cryst. (1994). A**50**, 455–461

Strip-Projection Approach to a New Model of the AlMnSi Icosahedral Quasicrystal

BY Y. F. CHENG* AND J. GJØNNES

Department of Physics and Center for Materials Research, University of Oslo, PO Box 1048 *Blindern,* 0316 *Oslo, Norway*

(*Received* 24 *June* 1992; *accepted* 17 *November* 1993)

Abstract

Recently, an approach to the atomic model of the AlMnSi quascrystalline phase has been proposed. Rhombohedra that differ from those used in the Penrose tiling were used to form an approximant. It gave a good approximation to the AlMnSi quasicrystal structure. In the present paper, a strip-projection approach to this model is implemented. It is demonstrated that the tiling, with the tile edges along the threefold axes of the icosahedral symmetry, can also be used to describe the structure of the AlMnSi icosahedral quasicrystal. The Mackay icosahedra are decorated at the vertices of the tiles.

1. Introduction

After the first discovery of an icosahedral quasicrystal (Shechtman, Blech, Gratias & Cahn, 1984), various models were proposed to describe its structure (Elser & Henley, 1985; Guyot & Audier, 1985; Yang & Kuo, 1986; Cahn, Gratias & Mozer, 1988*a*; Duneau & Oguey, 1989; Pan, Cheng & Li, 1990; Andersson, Lidin, Jacob & Terasaki, 1991). A generally accepted geometrical model for describing the quasiperiodicity and the symmetry of the quasicrystals has been the Penrose tiling (Penrose, 1974; Mackay, 1982). It consists of two different rohombohedra [a prolate rhombohedron (PR) and an oblate rhombohedron (OR)] as the building tiles, packed according to a special matching rule. However, the determination of atomic structure remains a principal problem. One of the approaches is to decorate atoms in the two kinds of Penrose tiles. An example shown by Elser & Henley (1985) is that the body-centred cubic (b.c.c.) structure of the crystalline approximant α-AlMnSi phase was decomposed into a periodic packing of the PR and OR, and its atomic decoration was proposed to be included in the icosahedral phase. Some models were proposed based on this approach (Henley & Elser, 1986; Guyot & Audier, 1985).

A different viewpoint was offered by Audier & Guyot (1988). From the similarity of intensity distribution in the diffraction patterns of both the α-AlMnSi phase and the quasicrystalline phase, they suggested that the Mackay icosahedron, which is a 54-atom cluster $[(AlSi)_{42}Mn_{12}]$ with icosahedral symmetry, is a common building block in both phases. Comparison of Patterson syntheses for both the phases (Cahn, Gratias & Mozer, 1988*b*) lends support to this assumption, *i.e.* a description of the AlMnSi quasicrystal as a packing of Mackay

*Present address: Institute of Physics, Chinese Academy of Sciences, PO Box 603, Beijing 100080, People's Republic of China.

©1994 International Union of Crystallography
Printed in Great Britain – all rights reserved

icosahedra. Several models based on this approach have been proposed (Audier & Guyot, 1988; Andersson *et al.*, 1991).

In a transmission-electron-microscopy (TEM) study of the precipitation process of industrial Al–Mn–Fe–Si alloys, Hansen, Gjønnes & Andersson (1989) found the icosahedral quasicrystal particles to be the first precipitates that subsequently transformed to the α phase. In this sequence, a new trigonal structure denoted α', which was interpreted as another packing of the Mackay icosahedra (Hansen & Gjønnes, 1992), was found as microdomains in contact with the α phase. The two structures, α and α', represent two kinds of rhombohedral unit cell, *viz* the OR corresponding to the primitive rhombohedral unit cell of the b.c.c. α phase and the complementary PR corresponding to the rhombohedral unit cell of the α' structure. Based on these experimental results, a modelling process that approached an atomic model of the AlMnSi icosahedral quasicrystal was proposed by Hansen & Gjønnes (1994) as a packing of the Mackay icosahedra in accordance with the two kinds of rhombohedra. The PR and OR (Figs. 1*a* and *b*) differ from the commonly used three-dimensional (3D) Penrose tiles in having a larger edge length of 10.88 Å (*versus* 4.6 Å for the Penrose tiles) and rhombohedral angles of 70.53° [$=\arccos(1/3)$] and 109.47° [$=180-70.53°$], which correspond to angles between triads in the icosahedron, whereas the Penrose tiles (Amman rhombohedra) have edges parallel to the fivefold axes. The size of the present set of tiles is such that the Mackay icosahedra can be accommodated on the vertices of the tiles and the inter-icosahedral distance in the α phase is preserved. A model with cubic symmetry built from the two types of tiles was shown to produce an atomic arrangement and diffraction patterns with near icosahedral symmetry and was hence suggested as an approximant to a true quasicrystalline structure; with reference to the α phase, it was called the secondary approximant of the AlMnSi quasicrystal. It is the purpose of the present study to investigate this further, in particular with regard to whether such a modelling process can be derived from a hypercubic lattice in six-dimensional (6D) space with a strip-projection approach.

2. 3D quasilattice and its Fourier transformation

In the present description of the AlMnSi icosahedral quasicrystal, ten equivalent threefold axes of the icosahedral symmetry are prominent while only six of them are independent. Let $\mathbf{A}_i$ ($i=1,...,10$) be the sums of three basic vectors $\mathbf{e}_i$ ($i=1,...,6$) of a 6D hypercubic lattice that are along the edges of the 6D hypercube unit cell with length $A_0=6.45$ Å in the case of the AlMnSi icosahedral quasicrystal; the projections of the $\mathbf{A}_i$ in both $E_\parallel$ and $E_\perp$ are along the ten threefold axes of the icosahedral symmetry. In the 6D Cartesian coordinate system, which is the combination of the Cartesian coordinates in both $E_\parallel$ and $E_\perp$ with basic vectors $\mathbf{E}_\parallel^x$, $\mathbf{E}_\parallel^y$, $\mathbf{E}_\parallel^z$ and $\mathbf{E}_\perp^x$, $\mathbf{E}_\perp^y$, $\mathbf{E}_\perp^z$, respectively, the $\mathbf{A}_i$ are expressed as

$$\begin{bmatrix} \mathbf{A}_1 \\ \mathbf{A}_2 \\ \mathbf{A}_3 \\ \mathbf{A}_4 \\ \mathbf{A}_5 \\ \mathbf{A}_6 \\ \mathbf{A}_7 \\ \mathbf{A}_8 \\ \mathbf{A}_9 \\ \mathbf{A}_{10} \end{bmatrix} = \frac{A_0}{[2(1+\tau^2)]^{1/2}} \begin{bmatrix} \tau^2 & \tau^2 & -\tau^2 & -1/\tau & -1/\tau & 1/\tau \\ \tau^2 & -\tau^2 & \tau^2 & -1/\tau & 1/\tau & -1/\tau \\ -\tau^2 & \tau^2 & \tau^2 & 1/\tau & -1/\tau & -1/\tau \\ \tau^3 & \tau & 0 & 1/\tau^2 & 1 & 0 \\ \tau & 0 & \tau^3 & 1 & 0 & 1/\tau^2 \\ 0 & \tau^3 & \tau & 0 & 1/\tau^2 & 1 \\ \tau^2 & \tau^2 & \tau^2 & -1/\tau & -1/\tau & -1/\tau \\ \tau^3 & -\tau & 0 & 1/\tau^2 & -1 & 0 \\ -\tau & 0 & \tau^3 & -1 & 0 & 1/\tau^2 \\ 0 & \tau^3 & -\tau & 0 & 1/\tau^2 & -1 \end{bmatrix} \begin{bmatrix} \mathbf{E}_\parallel^x \\ \mathbf{E}_\parallel^y \\ \mathbf{E}_\parallel^z \\ \mathbf{E}_\perp^x \\ \mathbf{E}_\perp^y \\ \mathbf{E}_\perp^z \end{bmatrix}, \quad (1)$$

where $\tau=(1+5^{1/2})/2$. As for the threefold axes in 3D space, of these ten equivalent vectors only six are independent. Therefore, six of them could be chosen as the basic vectors for specifying the hypercubic lattice, although the 6D unit cell specified by such basic vectors is not a hypercube but the 6D hypercubic lattice is unchanged. There are several different choices of the basic vector sets from $\mathbf{A}_i$ that are equal but with differently oriented unit cells. For a tiling in 3D space with its tile edges along all the ten equivalent threefold axes, the projections of ten $\mathbf{A}_i$ in $E_\parallel$ and $E_\perp$ are taken as the basic vectors in both spaces. Therefore, if a corresponding 6D unit cell is defined as specified by all ten vectors $\mathbf{A}_i$, it contains all the differently oriented unit cells specified by different basic vector sets. In the 3D Cartesian coordinate

systems, the basic vectors are expressed as

$$\begin{cases} \mathbf{a}_\parallel^1 = A(1,1,-1), & \mathbf{a}_\parallel^4 = A(\tau,1/\tau,0), \\ \mathbf{a}_\parallel^2 = A(1,-1,1), & \mathbf{a}_\parallel^5 = A(1/\tau,0,\tau), \\ \mathbf{a}_\parallel^3 = A(-1,1,1), & \mathbf{a}_\parallel^6 = A(0,\tau,1/\tau), \\ \mathbf{a}_\parallel^7 = A(1,1,1), & \mathbf{a}_\parallel^9 = A(-1/\tau,0,\tau), \\ \mathbf{a}_\parallel^8 = A(\tau,-1/\tau,0), & \mathbf{a}_\parallel^{10} = A(0,\tau,-1/\tau). \end{cases} \quad (2a)$$

and

$$\begin{cases} \mathbf{a}_\perp^1 = B(-1,-1,1), & \mathbf{a}_\perp^4 = B(1/\tau,\tau,0), \\ \mathbf{a}_\perp^2 = B(-1,1,-1), & \mathbf{a}_\perp^5 = B(\tau,0,1/\tau), \\ \mathbf{a}_\perp^3 = B(1,-1,-1), & \mathbf{a}_\perp^6 = B(0,1/\tau,\tau), \\ \mathbf{a}_\perp^7 = B(-1,-1,-1), & \mathbf{a}_\perp^9 = B(-\tau,0,1/\tau), \\ \mathbf{a}_\perp^8 = B(1/\tau,-\tau,0), & \mathbf{a}_\perp^{10} = B(0,1/\tau,-\tau), \end{cases} \quad (2b)$$

where $A = A_0\tau^2/[2(1+\tau^2)]^{1/2} = 6.28$ Å and $B = A_0/\{\tau[2(1+\tau^2)]^{1/2}\} = 1.48$ Å. The configurations of all basic vectors are shown in Figs. 2(*a*) and (*b*). The length of the $\mathbf{a}_\parallel^i$ ($i = 1,2,...,10$) is 10.88 Å, which is the edge length of the PR and OR. The correspondence of the configuration of the $\mathbf{a}_\parallel^i$ and the $\mathbf{a}_\perp^i$ ($i = 1,...,10$) could also be derived from the icosahedral point symmetry.

According to the strip-projection method (Elser, 1985), the 3D quasilattice or the tiling is the projection of all the 6D hypercubic lattice points located inside a strip S onto $E_\parallel$. The tiles are spanned by three basic vectors in $E_\parallel$ and every combination of three basic vectors from ten $\mathbf{a}_\parallel^i$ forms a tile, which leads to in total $C_{10}^3 = 120$ different tiles in the present tiling. In addition to the ten different oriented PR and twenty OR there are three other distinct tiles with monoclinic prismoidal shapes [hereinafter denoted MR1, MR2 and MR3, with shapes as shown in Figs. 1(*c*), (*d*) and (*e*)]. In the present 3D tiling, there are 30 different orientations for each. Among them, MR1 and MR2 have appeared before in a quasiperiodic tiling with broken icosahedral symmetry derived by Socolar, Steinhardt & Levine (1985) from the so-called 'generalized dual method', which has only six independent basic vectors along six of the ten threefold axes. The matching rule for packing these tiles in the present description is determined by the orientation of the strip S in the 6D space, which is now parallel to $E_\parallel$.

To provide a description of the structure of the AlMnSi quasicrystal, the present tiling must have both quasiperiodicity and icosahedral symmetry. The former is ensured by the irrational orientation of the strip S within the 6D periodic lattice. The latter condition, which has been studied extensively (see review papers, *e.g.* Janssen & Janner, 1987), follows from the embedding of the periodic lattice in the higher-dimensional space and the symmetry of the projection window in the pseudo-space. The basic vectors in both $E_\parallel$ and $E_\perp$ are consistent with the icosahedral symmetry. The projection window in $E_\perp$ is taken as the projection of the unit cell specified by ten basic vectors $\mathbf{A}_i$ onto $E_\perp$: $W_\perp = \{\sum_{i=1}^{10} x_i a_\perp^i | -\frac{1}{2} < x_i < \frac{1}{2}\}$; it is an enneacontrahedron (Fig. 3; Kramer & Haase, 1989), which has icosahedral symmetry and is formed by packing all the 120 different rhombohedral tiles together without holes and overlaps. Therefore, the tiling obtained from this projection window does have icosahedral symmetry.

The Fourier transformation of the 3D quasilattice was calculated using the method of Elser (1986). As a simplification, the spherical approximation of the projection window was used in the present calculations, which does not change the symmetry of the Fourier transformation patterns. If all the quasilattice points in the 3D tiling contain the same atom or atom cluster (*viz* the Mackay icosahedron), the kinematical intensities of the diffraction peaks can be obtained by multiplying the atomic scattering factors of the atom or atom cluster by the amplitude factors that are the Fourier transformation of the projection

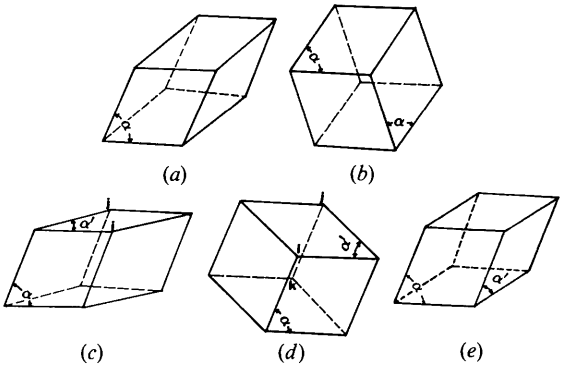

Fig. 1. Five different tiles in the 3D projected quasilattice: (*a*) prolate rhombohedron (PR); (*b*) oblate rhombohedron (OR); (*c*), (*d*) and (*e*) monoclinic prismoidal shapes (MR) 1, 2 and 3, respectively. Here, $\alpha = 70.53$ and $\alpha' = 41.83°$.

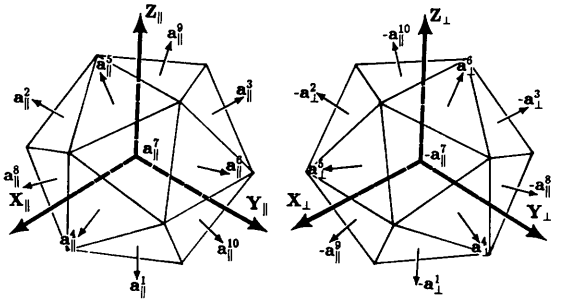

Fig. 2. Configurations of basic vectors $\mathbf{a}_\parallel^i$ and $\mathbf{a}_\perp^i$ ($i = 1,2,...,10$) in the physical space $E_\parallel$ and the pseudo-space $E_\perp$, respectively.

window. Fig. 4 shows a set of calculated Fourier transformation patterns of the quasiperiodic tiling derived above along its five-, three- and twofold axes, respectively, where the areas of the circles are proportional to the amplitude factors of the corresponding reciprocal vectors.

3. Approximants in AlMnSi alloys

So far, much work has been done with the approximants of the quasicrystals (*e.g.* Ishii, 1989; Dmitrienko, 1990; Li & Cheng, 1990; Niizeki, 1992). Changing the orientation of the strip S in the 6D space changes the matching rules of the tiles and results in a series of approximants with periodic packing of the tiles. The Fourier transformations of these approximant lattices are calculated by rotation of the reciprocal physical space $E_{\parallel}^{*}$ in 6D reciprocal space to an orientation parallel to the rotated strip (*e.g.* Elser & Henley, 1985; Mai, Tao, Zhang & Zeng, 1989; Cheng, Pan & Li, 1992). As mentioned in the *Introduction*, it is our purpose to derive all the quasicrystalline approximants proposed by Hansen & Gjønnes (1992, 1993) in their modelling process of the AlMnSi alloys from the strip-projection viewpoint.

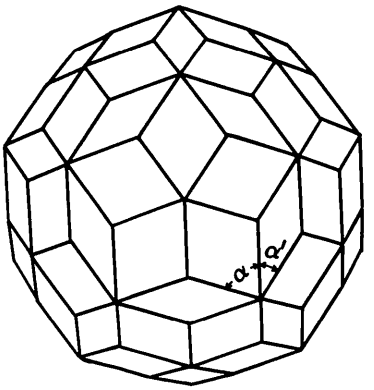

Fig. 3. Enneacontrahedron with icosahedral symmetry.

(i) α-AlMnSi *phase*

The α-AlMnSi phase has a b.c.c. or nearly b.c.c. structure with space group $Im3$ or $Pm3$ and lattice parameter about 12.56 Å (Cooper, 1967; Cooper & Robinson, 1966). Its structure has a close relationship with the icosahedral phase of the same alloy, *viz* both contain Mackay icosahedra as the main building blocks of the structure. The primitive rhombohedral unit cell of the α phase is the OR tile in the present projected tiling. In this case, the $\mathbf{A}_i$ ($i = 1,...,6$) were used as the basic vectors and the corresponding strip S' was formed by moving the noncubic unit cell specified by these six basic vectors along a certain orientation:

$$\begin{bmatrix} S'_x \\ S'_y \\ S'_z \end{bmatrix} = \begin{bmatrix} 1 & 1 & 0 & 0 & 0 & 0 \\ 1 & 0 & 1 & 0 & 0 & 0 \\ 0 & 1 & 1 & 0 & 0 & 0 \end{bmatrix} \begin{bmatrix} \mathbf{A}_1 \\ \mathbf{A}_2 \\ \mathbf{A}_3 \\ \mathbf{A}_4 \\ \mathbf{A}_5 \\ \mathbf{A}_6 \end{bmatrix}. \quad (3a)$$

S' is now rational to the 6D periodic lattice and perpendicular to $\mathbf{A}_4$, $\mathbf{A}_5$ and $\mathbf{A}_6$. This leads to a periodic packing of OR spanned by only ($\mathbf{a}_{\parallel}^{1}$,$\mathbf{a}_{\parallel}^{2}$,$\mathbf{a}_{\parallel}^{3}$), which is obviously the b.c.c. lattice of the α-AlMnSi phase. Fig. 5 shows the calculated Fourier transformation patterns along the [τ10], [111] and [100] directions, respectively, which are the same as those calculated from the phason-defected Penrose tiling.

(ii) α' *phase*

The α' trigonal structure was first found as the domain in contact with the α phase in precipitate particles during the transformation of the icosahedral phase to the α phase (Hansen & Gjønnes, 1992). Later, it was found as precipitate particles formed directly from the supersaturated aluminium solid solutions (Cheng, Hansen, Gjønnes & Wallenberg, 1992). As for the α phase, the strip

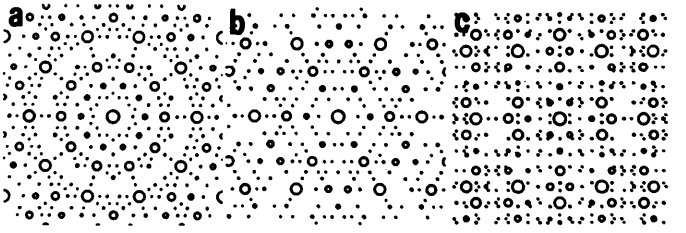

Fig. 4. Calculated Fourier transformation patterns of the 3D projected quasiperiodic tiling along (*a*) a fivefold axis, (*b*) a threefold axis and (*c*) a twofold axis.

was rotated to a rational orientation:

$$\begin{bmatrix} S''_x \\ S''_y \\ S''_z \end{bmatrix} = \begin{bmatrix} 0 & -1 & 1 & 4 & 0 & 0 \\ 0 & -1 & 1 & 0 & 0 & 0 \\ 0 & 1 & 1 & 0 & 0 & 0 \end{bmatrix} \begin{bmatrix} \mathbf{A}_1 \\ \mathbf{A}_2 \\ \mathbf{A}_3 \\ \mathbf{A}_4 \\ \mathbf{A}_5 \\ \mathbf{A}_6 \end{bmatrix}. \quad (3b)$$

S'' is now perpendicular to $\mathbf{A}_1$, $\mathbf{A}_5$ and $\mathbf{A}_6$. This causes the periodic packing of only PR $(\mathbf{a}_\parallel^2, \mathbf{a}_\parallel^3, \mathbf{a}_\parallel^4)$, which corresponds to the trigonal rhombohedron of the α' structure. The calculated patterns along a pseudo-fivefold axis and the [111] and $[1\bar{1}0]$ directions, are given in Fig. 6. The orientation relationship with the icosahedral quasicrystal should be the $[1\bar{1}0]_{\alpha'}$ parallel to a twofold axis of quasicrystal and the $[111]_{\alpha'}$ parallel to a threefold axis.

(iii) *Secondary cubic approximant*

In the secondary cubic approximant constructed by Hansen & Gjønnes (1992, 1994), the unit cell contains four PR and four OR with a lattice parameter of about 20.33 Å and the space group $Pa3$. Its optical diffraction pattern gave a good approximation to the diffraction patterns of the quasicrystal (Fig. 7*b*). This secondary approximant is obtained by taking the orientation of the strip S''' as follows:

$$\begin{bmatrix} S'''_x \\ S'''_y \\ S'''_z \end{bmatrix} = \begin{bmatrix} 1 & 0 & 0 & 1 & 0 & 0 \\ 0 & 0 & 1 & 0 & 0 & 1 \\ 0 & 1 & 0 & 0 & 1 & 0 \end{bmatrix} \begin{bmatrix} \mathbf{A}_1 \\ \mathbf{A}_2 \\ \mathbf{A}_3 \\ \mathbf{A}_4 \\ \mathbf{A}_5 \\ \mathbf{A}_6 \end{bmatrix}. \quad (3c)$$

The projected tiling in $E_\parallel$ is the same as Hansen & Gjønnes (1992, 1994) constructed in their paper, *viz* the periodic packing of both PR and OR but without MRs. Fig. 7(*a*) shows the calculated patterns along a pseudo-fivefold axis and Fig. 7(*b*) is the optical diffraction pattern from the paper by Hansen & Gjønnes (1994). The similarity between the two patterns is apparent.

Beyond this secondary cubic approximant, PR and OR cannot fill the whole space and some MRs are needed. This results in faults in the proposed modelling process. Differently oriented tiles must be taken into the tiling, which corresponds to the involvement of differently oriented unit cells in the 6D space.

4. Atomic decoration of the tiles

In the AlMnSi alloys, the atomic structure of the most important approximant, the α phase, is well

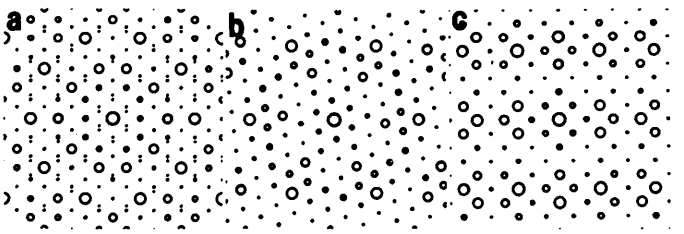

Fig. 5. Calculated patterns of the approximant α lattice along (*a*) a pseudo-fivefold direction, (*b*) the [100] direction and (*c*) the [111] direction.

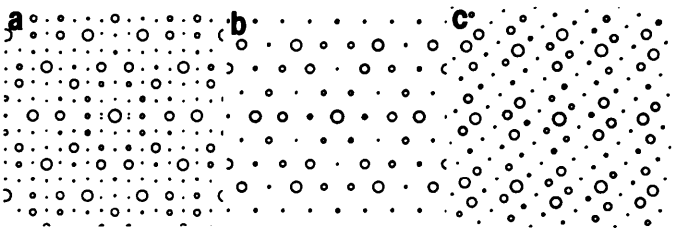

Fig. 6. Calculated patterns of the trigonal approximant α' structure along (*a*) a pseudo-fivefold axis, (*b*) the $[1\bar{1}0]$ direction and (*c*) the [111] direction.

determined. It gives the atomic decoration of OR, that is, the Mackay icosahedra decorated on its vertices with their threefold axes parallel to the edge directions of the rhombohedra and with some 'glue' atoms between the Mackay icosahedra. The structure of the α' trigonal lattice that appears in the present treatment as an alternative approximant as well as the α phase in the same alloy was believed to have the Mackay icosahedra located at the vertices; it gives the decoration of PR. Then, in the 3D tiling, all the Mackay icosahedra have the same orientation, *i.e.* the threefold axes of the Mackay icosahedra coincide with the edge directions of the tiles. For MRs, it should be noted that the distances between some of the vertices such as *i* and *j* in MR1 (Fig. 1*c*) or *i* and *k* in MR2 (Fig. 1*d*) and so on are too short to decorate the complete Mackay icosahedra at all these vertices. Hansen & Gjønnes (1994) indicated that the third-order approximant will contain certain defects where some of the Mackay icosahedra must be removed. In the model proposed by Andersson *et al.* (1991), many Mackay icosahedra are cut in order to get a close packing. It seems that the atomic decoration of MRs should be treated in a similar way; that is, by removing some of the Mackay icosahedra from some quasilattice points or by cutting some of these Mackay icosahedra to fit the shapes of those tiles.

5. Discussion

The tiling that is proposed here differs from the commonly used 3D Penrose tiling but is derived from the same 6D hypercubic lattice and might be regarded as a subquasilattice of the Penrose tiling. Actually, the basic difference between the present approach and the procedure leading to the Penrose tiling lies in the choice of projection window in $E_\perp$, whose volume equals the density of the quasilattice points of the tiling (Elser, 1986). The tria-contrahedral window for the Penrose tiling has a larger volume than that of the present ennea-contrahedral window; $V_{\text{ennea}} = 0.888 V_{\text{tria}}$. A remaining question is whether the present tiling can be constructed without overlap of the tiles; it seems that this is the case but no mathematical proof has yet been presented. The atomic decoration of the tiles has not been solved completely. It is seen that the OR as well as the PR can accommodate Mackay icosahedra, but some additional 'glue' atoms must be included in these. The decoration of MRs will need special consideration, *e.g.* by study of the approximants beyond the second.

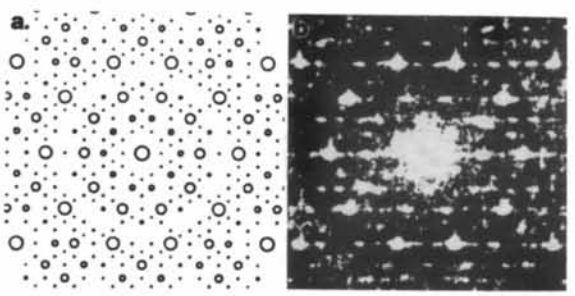

Fig. 7. (*a*) Calculated patterns of the cubic secondary approximant along a pseudo-fivefold axis and (*b*) the optical diffraction pattern of a projected model along the same direction of the cubic secondary approximant model (from Hansen & Gjønnes, 1992).

Some experimental observations support the present tiling, especially the OR and PR tiles. In a TEM study of the precipitation process of the industrial Al3003 alloys (Cheng, Hansen *et al.*, 1992), evidence of three different nucleation paths of dispersoid particles was found, *viz* (1) the icosahedral quasicrystal formed first from aluminium solid solution and then transformed to the α phase upon further heat treatment, (2) the α-phase particles with relatively perfect structure formed directly from aluminium solid solution and (3) the α' particles with imperfect trigonal structure also formed directly from aluminium solid solution. All these particles have Mn/Fe-containing Mackay icosahedra as their basic atomic building blocks. This suggested that three different nucleation paths originate from the Mackay icosahedra in the aluminium solid solution that, predicted from the theoretical calculation (Boyer & Broughton, 1990), are energetically favoured over other atomic clusters during the solidification process. On heat treatment, the different packings of the Mackay icosahedra result in the different nucleation paths. When Mackay icosahedra are packed only on the OR, the α-phase particles are formed; when they are packed only on the PR, the trigonal lattice particles are formed. When both packings are mixed together, particles with icosahedral quasicrystal structure are formed. But the Mackay icosahedra could not be packed only on the MRs because there is not enough space in these tiles for decorating Mackay icosahedra; this is the reason why no precipitate was found to have the structures of MRs. On the other hand, since the whole space cannot be filled by PR and OR, the gaps between them are filled by MRs.

The authors thank Hydro Aluminium a.s. for financial support and V. Hansen for useful discussions. YFC is grateful to the Royal Norwegian Council for Scientific and Industrial Research (NTNF) for a postdoctoral research fellowship.

References

ANDERSSON, S., LIDIN, S., JACOB, M. & TERASAKI, O. (1991). *Angew. Chem. Int. Ed. Engl.* **30**, 754–758.

AUDIER, M. & GUYOT, P. (1988). *Quasicrystalline Materials. Proceedings of the ILL/CODEST Workshop*, edited by C. JANOT & J. M. DUBOIS, pp. 181–194. Singapore: World Scientific.
BOYER, L. L. & BROUGHTON, J. Q. (1990). *Phys. Rev. B*, **42**, 11461–11468.
CAHN, J. W., GRATIAS, D. & MOZER, B. (1988*a*). *J. Phys. (Paris)*, **49**, 1225–1233.
CAHN, J. W., GRATIAS, D. & MOZER, B. (1988*b*). *Phys. Rev. B*, **38**, 1638–1642.
CHENG, Y. F., HANSEN, V., GJØNNES, J. & WALLENBERG, R. L. (1992). *J. Mater. Res.* **7**, 3235–3241.
CHENG, Y. F., PAN, G. Z. & LI, F. H. (1992). *Phys. Status. Solidi B*, **170**, 47–55.
COOPER, M. (1967). *Acta Cryst.* **23**, 1106–1107.
COOPER, M. & ROBINSON, K. (1966). *Acta Cryst.* **20**, 614–617.
DMITRIENKO, V. E. (1990). *J. Phys. (Paris)*, **51**, 2712–2732.
DUNEAU, M. & OGUEY, C. (1989). *J. Phys. (Paris)*, **50**, 135–146.
ELSER, V. (1985). *Phys. Rev. B*, **32**, 4892–4898.
ELSER, V. (1986). *Acta Cryst.* A**42**, 36–43.
ELSER, V. & HENLEY, C. L. (1985). *Phys. Rev. Lett.* **55**, 1883–1886.
GUYOT, P. & AUDIER, M. (1985). *Philos. Mag.* B**52**, L15–L19.
HANSEN, V. & GJØNNES, J. (1992). *Micron Microsc. Acta*, **23**, 175–176.
HANSEN, V. & GJØNNES, J. (1994). In preparation.
HANSEN, V., GJØNNES, J. & ANDERSSON, B. (1989). *J. Mater. Sci. Lett.* **8**, 823–826.
HENLEY, C. L. & ELSER, V. (1986). *Philos. Mag.* B**53**, L59–L66.
ISHII, Y. (1989). *Phys. Rev. B*, **39**, 11862–11871.
JANSSEN, T. & JANNER, A., (1987). *Adv. Phys.* **36**, 519–624.
KRAMER, P. & HAASE, R. W. (1989). In *Aperiodicity and Order* 2: *Introduction to the Mathematics of Quasicrystals*, edited by MARKO V. JARIĆ. New York: Academic Press.
LI, F. H. & CHENG, Y. F. (1990). *Acta Cryst.* A**46**, 142–149.
MACKAY, A. L. (1982). *Physica. (Utrecht)*, A**114**, 609–613.
MAI, Z. H., TAO, S. Z., ZHANG, B. S. & ZENG, L. Z. (1989). *J. Phys. Condens. Matter*, **1**, 2465–2471.
NIIZEKI, K. (1992). *J. Phys. A*, **25**, 1843–1854.
PAN, G. Z., CHENG, Y. F. & LI, F. H. (1990). *Phys. Rev. B*, **51**, 3401–3405.
PENROSE, R. (1974). *Bull. Inst. Math. Appl.* **10**, 266–271.
SHECHTMAN, D., BLECH, I., GRATIAS, D. & CAHN, J. W. (1984). *Phys. Rev. Lett.* **53**, 1951–1953.
SOCOLAR, J. E. S., STEINHARDT, P. J. & LEVINE, D. (1985). *Phys. Rev. B*, **32**, 5547–5550.
YANG, Q. B. & KUO, K. H. (1986). *Philos. Mag.* B**53**, L115–L121.

Acta Cryst. (1994). A**50**, 461–467

The Temperature Dependence of the Reflection Intensities of the Modulated Composite Structure $Hg_{0.776}$(BEDT-TTF)SCN

BY MARK R. PRESSPRICH, CORNELIS VAN BEEK* AND PHILIP COPPENS

Department of Chemistry, State University of New York at Buffalo, Buffalo, NY 14214, *USA*

(*Received* 3 *November* 1992; *accepted* 2 *December* 1993)

Abstract

The temperature dependence between 30 and 300 K of the intensities of 24 reflections of the column-composite structure $Hg_{0.776}$(BEDT-TTF)SCN [Wang, Beno, Carlson, Thorup, Murray, Porter, Williams, Maly, Bu, Petricek, Cisarova, Coppens, Jung, Whangbo, Schirber & Overmyer (1991). *Chem. Mater.* **3**, 508–513; BEDT-TTF = 3,4,3′,4′-bis(ethylenedithio)-2,2′,5,5′-tetrathiafulvalene] has been analyzed in terms of a model including phason temperature factors. The temperature dependence of the main and first-order satellite reflections is reasonably well reproduced in a refinement with 236 observations and four variables. The results are interpreted in terms of a temperature independence of the static displacement amplitudes. The room-temperature r.m.s. phason fluctuations of the mercury sublattice are 50 (2)°. This value implies that the *mean* mercury displacement amplitude will increase by ~60% on lowering of the temperature to within the liquid-helium range. The thermal contraction on cooling is the same for the two sublattices.

Introduction

For a modulated crystal, the usual description of the effect of atomic thermal motion on the reflection intensities must be modified by the introduction of Debye–Waller factors that vary from unit cell to unit cell along the modulation-vector direction, as the translational symmetry in this direction no longer exists. The temperature-factor modulation can be described by a Fourier series, the form of which follows from superspace-group theory (Yamamoto, 1982).

In addition, the phase and amplitude of the modulation can fluctuate. Such modes are thermally excited at quite low temperatures. The temperature-factor theory of phasons and amplitudons was introduced by Overhauser (1971) and further developed by Axe (1980). Perez-Mato & Madariaga (1990)

* Current address: University of Twente, The Netherlands.

©1994 International Union of Crystallography
Printed in Great Britain – all rights reserved